JOURNAL OF THE OPTICAL SOCIETY OF AMERICA VOLUME 61, NUMBER 9 SEPTEMBER 1971

# Spatial-Frequency Channels in Human Vision*

MURRAY B. SACHS†
*Navy Underwater Sound Laboratory, New London, Connecticut 06320*

JACOB NACHMIAS
*Department of Psychology, University of Pennsylvania, Philadelphia, Pennsylvania 19104*

AND

JOHN G. ROBSON
*The Physiological Laboratory, Cambridge University, Cambridge, England*

(Received 15 June 1970; revision received 25 March 1971)

Psychometric functions were determined concurrently for detection of simple gratings (luminance sinusoidally modulated with spatial frequency $f$) and complex gratings (luminance modulated by the sum of two sinusoids, with frequencies $f$ and $f'$). Results were used to test the hypothesis that the two components of a complex grating may be detected independently. In an extensive experiment with $f=14$ cycles/deg, the independence hypothesis was consistently rejected only when $f/f'=\frac{5}{4}$ or $\frac{4}{5}$, but rarely rejected when the value of $f/f'$ lay outside this range. In other experiments, $f$ was between 1.9 and 22.4 cycles/deg. All results are compatible with the assumption that the human visual system contains sensory channels, each selectively sensitive to different narrow ranges of spatial frequencies, whose outputs are detected independently.

INDEX HEADING: Vision.

Over the past decade, many investigators have been studying the human visual system with stimuli whose luminance distributions are sinusoidal functions of space or time, or even both.[1–3] The primary motivation behind the use of this class of stimuli has been the hope that results could be conveniently interpreted within the framework of linear-systems analysis. In attributing various features of empirical results to optical and neural factors, many investigators have treated the visual system as a single filter, made up as a cascade of

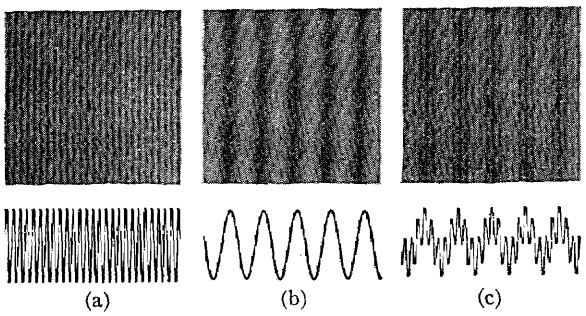


FIG. 1. Simple gratings (a) and (b), complex grating (c), and corresponding luminance waveforms. The amplitudes of the two components of the complex gratings are one half the amplitudes for the corresponding simple gratings so that the peak-to-trough amplitudes of all three patterns are the same. In our experiments, the frequencies (cycles/deg) of these gratings were: (a), $f=14$; (b), $f'=2.8$.

optical and neural filters.[1,4] Psychophysically determined functions relating contrast sensitivity to spatial frequency have been taken to be modulation transfer functions of this single visual filter.

Campbell and Robson[5] suggested a rather different model for the detection of sinusoidal gratings. According to this model, the visual system contains a number of neural channels each selectively sensitive to a different range of spatial frequencies. It has since been demonstrated electrophysiologically that some single units in the visual system respond to gratings moving continuously over their receptive fields only if the gratings' spatial frequencies lie within a limited range of values; the range is different for different units. For example, such frequency-selective units have been found in the cat by Enroth-Cugell and Robson[6] and in monkeys by Campbell *et al.*[7] Strong evidence for the existence of similar tuned elements in man comes from psychophysical experiments involving adaptation of gratings.[8–10] Our experiments indicate that these spatial-frequency channels not only exist in man but that the outputs of different channels are detected independently.

## EXPERIMENTAL PARADIGM AND CONCEPTUAL FRAMEWORK

We determined concurrently the psychometric functions for the detection of simple and complex gratings. Examples of such gratings are shown in Fig. 1. The luminance of a simple grating of spatial frequency $f$ is sinusoidally modulated along the horizontal dimension with a spatial frequency $f$

$$L(x)=L_0[1+m\sin(2\pi fx+\phi)]. \quad (1)$$

The modulation, $m$, of a simple grating is equal to its contrast, where contrast$=(L_{\max}-L_{\min})/2L_0$. The luminance of a complex grating is modulated by the sum of two sinusoids, with frequencies $f$ and $f'$,

$$L(x)=L_0[1+m\sin(2\pi fx+\phi)+m'\sin(2\pi f'x+\phi')]. \quad (2)$$

The space-average luminance, $L_0$, was constant at all

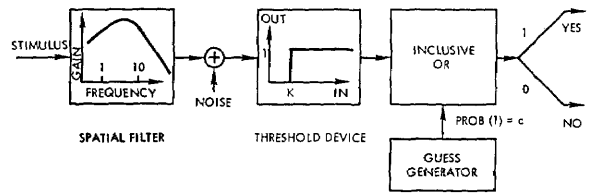


FIG. 2. Block diagram of the single-channel model.

times, regardless of the presence of any gratings. Note that for either $m$ or $m'$ equal to zero, a complex grating reduces to a simple grating at frequency $f'$ or $f$, respectively. The luminance waveforms for the simple and complex gratings are also shown in Fig. 1. For simple gratings at frequency $f$, as well as for complex gratings with components at $f$ and $f'$, the probability of detection was estimated as a function of $m$, the modulation of the sinusoid at frequency $f$. We shall refer to these estimated functions as simple and complex psychometric functions, respectively. The modulation $m'$ of the sinusoid at $f'$ in the complex grating was constant throughout an experimental session.

In consideration of the results of these experiments, it will be convenient to keep in mind two different models of the grating-detection process. Idealized block diagrams of these models are shown in Figs. 2 and 3. In the single-channel model (Fig. 2), the signal (i.e., the luminance distribution) is passed through a single spatial filter. Noise is added to the filter output to represent the uncertainty of the detection process. The noisy filter output is then passed through a threshold device. In the multiple-channel model (Fig. 3), the signal is passed through a parallel bank of narrow-band filters; independent noise is added to the filter outputs; the noisy signals are then detected by separate threshold devices. The signal will be detected if the threshold of any channel is exceeded. In both models we have added a guessing mechanism, which generates a "yes" response with some probability $c$, without regard to stimulus information.

Let us consider some predictions that result from these two models. For this purpose, it will be useful to

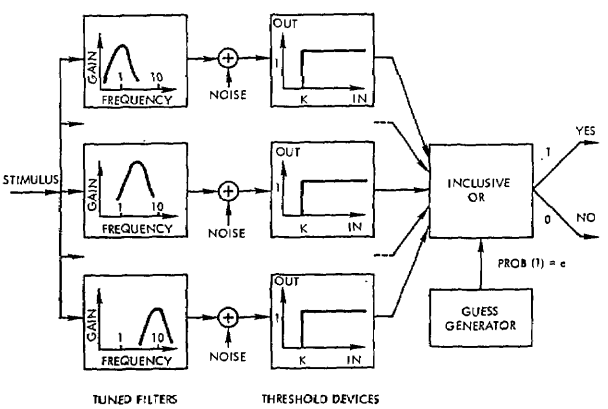


FIG. 3. Block diagram of the multiple-channel model.

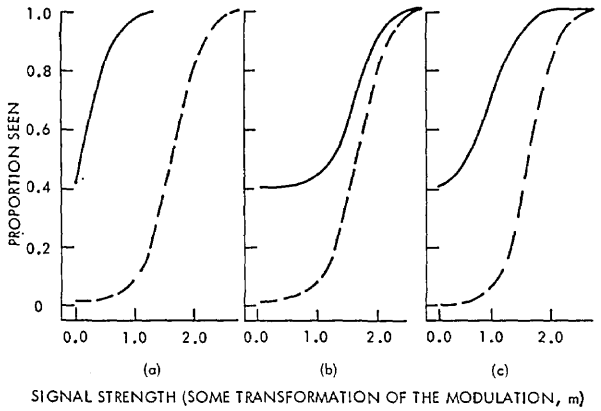


FIG. 4. Hypothetical complex psychometric functions resulting from the given simple psychometric function and (a), single-channel model; (b), the multi-channel model in the case where the two complex grating components are detected by completely separate channels; (c), the multiple-channel model in the case where one component is detected by two channels and the other component by only one of these channels. Dotted lines are simple psychometric functions and are the same for all cases; solid lines are complex psychometric functions for one value of $m'$.

introduce some additional notation:

$Y \equiv$ subject responds "Yes; I detect a grating."
$N \equiv$ subject responds "No; I don't detect a grating."
$T_i \equiv$ threshold of channel $i$ is exceeded.
$\bar{T}_i \equiv$ threshold of channel $i$ is not exceeded.
$P(A|B) \equiv$ probability of the occurrence of event $A$ conditioned on the occurrence of event $B$. For example, $P(Y|m,m') \equiv$ probability of response "yes," given that a grating with modulations $m$ and $m'$ at frequencies $f$ and $f'$ is presented.

Now let us suppose that the single-channel model were correct. Suppose further that for the single channel, the probability of detecting a complex grating were some function, $F$, of a linear combination of either the modulations $m$ and $m'$, or of some transformation of those modulations; that is,

$$P(Y|m,m') = F[aG(m) + a'G(m')], \tag{3}$$

where $G(\cdot)$ is some transformation, and $a$ and $a'$ are coefficients whose values depend on frequencies $f$ and $f'$. If, for example, the detector were a peak-to-peak detector of the modulation and suitable values were chosen for $f/f'$, and $\phi - \phi'$, $G(\cdot)$ would be a linear transformation.[11] If it were an average-power detector, $G(\cdot)$ would be a square law regardless of the frequencies and phases of the component sinusoids, provided that $f \neq f'$. For $m' = 0$, the complex grating reduces to a simple grating of frequency $f$. Then, if $P(Y|m,0)$ is the probability of detecting such a grating at modulation $m$, we have

$$P(Y|m,0) = F[aG(m) + a'G(0)]. \tag{4}$$

Since $m'$ is fixed, $G(m')$ and $G(0)$ in Eqs. (3) and (4) are merely different constants. Consequently if we plot simple and complex psychometric functions vs the transformed modulation $G(m)$, the complex psychometric function will be a parallel-shifted version of the simple psychometric function. The shift is leftward, of magnitude $a'[G(m') - G(0)]$. For the peak-to-peak detector, the abscissa would be proportional to the amplitude $m$; for the average-power detector, it would be proportional to $m^2$. An example of such a transformation is shown in Fig. 4(a). The intercept of the complex psychometric function with the ordinate ($m = 0$) is equal to the probability of detecting a simple grating of frequency $f'$. Because, for given values of $f$ and $f'$, this probability depends on the modulation $m'$, a family of complex psychometric functions would be generated by varying this modulation.

Next, let us consider the multiple-channel model. In the simplest case, the separation between $f$ and $f'$, relative to the bandwidth of each channel, is sufficiently great so that the channel (or channels) that detects $f$ does not detect $f'$ and vice versa. Then we have

$$P(T_1|m,m') = P(T_1|m,0) \equiv P(T_1|m),$$

and

$$P(T_2|m,m') = P(T_2|0,m') \equiv P(T_2|m'),$$

where the subscripts 1 and 2 refer to the channels most sensitive to frequencies $f$ and $f'$, respectively. On any one trial, the observer will respond "no" if, and only if, the threshold of neither channel 1 nor 2 is exceeded and the guessing mechanism generates a "no" response. Because there is only this one circumstance that will produce a "no" response, it is easier to derive expressions for the probabilities of not detecting various simple and complex gratings than for the probabilities of detecting them. Because the three events whose joint occurrence produces a "no" response are stochastically independent, the probability of "no" is simply the product of the probabilities of the three events. We can then write immediately the probabilities of not detecting the complex grating $P(N|m,m')$ and the two related simple gratings, $P(N|m,0)$ and $P(N|0,m')$,

$$P(N|m,m') = P(\bar{T}_1|m)P(\bar{T}_2|m')(1-c) \tag{5}$$

$$P(N|m,0) = P(\bar{T}_1|m)P(\bar{T}_2|0)(1-c) \tag{6}$$

$$P(N|0,m') = P(\bar{T}_1|0)P(\bar{T}_2|m')(1-c). \tag{7}$$

Then, for all values of $m$, and for $m' =$ a constant,

$$\frac{P(N|m,m')}{P(N|m,0)} = \frac{P(\bar{T}_2|m')}{P(\bar{T}_2|0)} = \text{a constant} \leq 1. \tag{8}$$

Thus, the probability of not detecting the complex grating is merely proportional to the probability of not detecting the corresponding simple grating at frequency $f$. By manipulation of Eqs. (5)–(7), the constant of

proportionality can be shown to be equal to the ratio of the probability of not detecting the simple grating at frequency $f'$ to the probability of not making a false alarm, that is, $P(N|0,m')/P(N|0,0)$. Note that this prediction requires no additional assumption about how $P(\bar{T}_1|\cdot)$ and $P(\bar{T}_2|\cdot)$ vary with $m$ and $m'$.

In Fig. 4(b), we show an example of the complex psychometric function generated by the assumption that $f$ and $f'$ are detected by totally separate channels. For convenience, we have shown a case where the false-alarm rate is zero. The probability of detecting a grating at frequency $f'$ alone ($m=0$) is 0.4 here or, equivalently, $P(N|0,m')=0.6$. Therefore, if we set the probability of not making a false alarm equal to 1, the ratio of the probabilities of not detecting the complex grating and the related simple grating at frequency $f$ is 0.6 for all values of $m$. Because the value of this ratio is determined by $P(N|0,m')$, a whole family of complex psychometric functions can be generated by setting $m'$ [and hence, $P(N|0,m')$] to different values.

The difference between the complex psychometric functions generated by these two models is striking. For instance, in the separate-channels case of the multiple-channel model [Fig. 4(b)], the detection probability is essentially constant in the signal range 0 to 0.5. In this range the complex psychometric function for the single-channel model [Fig. 4(a)] grows from 0.4 to 0.85.

However, suppose the separation between frequencies $f$ and $f'$ is small relative to the bandwidths of the several channels postulated in the multiple-channel model. In that case, which we will consider in greater detail in the Discussion section and in the Appendix, no simple relation exists between psychometric functions for simple and complex gratings. One possible set of psychometric functions for this case is shown in Fig. 4(c). As might be anticipated, the more similar the channels' sensitivities are to the two frequencies, the harder it is to discriminate between the predictions of the multiple- and single-channel models.

On the other hand, we have shown that for $f$ and $f'$ sufficiently different the multiple-channel model leads to predictions that are both easy to test and markedly different from those of the single-channel model. For these reasons, we shall use our results primarily to test the validity of the multiple-channel model in this simplest stimulus situation.

## METHODS

### A. Stimulus Presentation

Simple and complex gratings were generated on a cathode-ray tube with a P31 phosphor as described by Campbell and Robson.[5] They were presented for discrete periods of 760 ms, except in a few experiments performed to determine whether a shorter stimulus duration (108 ms) would significantly affect our results. (It did not.) The uniform luminance of the screen in the absence of any gratings was the same as the space-average luminance of all the gratings, approximately 20 mL. The face of the tube filled a square hole, $2\frac{1}{4}°$ on a side, in a large cardboard screen, which was illuminated so as nearly to match the CRT in luminance and color. In all of our experiments, $f$ and $f'$ were in the ratio of small integers. The oscillator producing one frequency was driven by the other oscillator in such a way as to maintain a constant phase relationship between the two sinusoids during stimulus presentation. For each pair of $f$ and $f'$ values, the relative phase was chosen that maximized the value of the largest peak-to-trough difference in the luminance distribution of the complex gratings.[11]

### B. Procedure

All psychometric functions were determined from one hundred observations per point. In any experimental session, the values of $f$, $f'$, and $m'$ were held constant. Simple and complex gratings with various values for the modulation $m$ were presented in a pseudorandom sequence of trials (method of constant stimuli). Also included were catch trials (no grating presented) and trials on which the sinusoid of frequency $f'$ was presented alone. In a few experimental sessions, only simple psychometric functions were determined.

The observer was seated 240 cm from the display, which he viewed binocularly, fixating an opaque spot on the face of the CRT. The display and the observer were shielded from room lights by a thick black curtain. The observer pressed a microswitch to initiate a trial; he responded "yes" if he saw a change from the constant luminance display and "no" if he did not. It is important to remember that the observer was asked only whether he saw a change from constant luminance, not what the stimulus was. This is a simple detection task, not a discrimination task.

### C. Observers

Two observers participated in the experiments reported here, for a period of three months. Observer MS was one of the investigators and was fully aware of the goals and progress of the research. The other observer (MR) was given only very limited knowledge of the research goals. Both observers worked three to five 1-h sessions per week. Observer MS was optically corrected for 20–20 acuity. MR was not optically corrected and had severe astigmatism.

## RESULTS

### A. Psychometric Functions for Simple Gratings

The major objective of this investigation was the analysis of related simple and complex psychometric functions. To minimize the effects of day-to-day

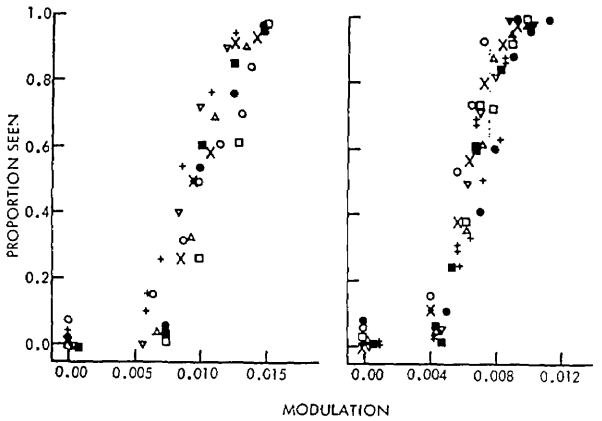


FIG. 5. Simple psychometric functions for $f=14$ cycles/deg. Each symbol represents results obtained on a different day during the period 21 March–27 May 1969. Left panel, O:MS; right panel, O:MR.

variability, we measured a pair of related functions in each session. Nevertheless, it is interesting to note that this source of variability proved to be smaller than we had anticipated. Figure 5 shows psychometric functions for $f=14$ cycles/deg, measured during the period 21 March–27 May 1969 with both observers. These results are strikingly stable; the modulation yielding 50% "yes" responses varied by less than a factor of 1.5.

Figure 6 shows examples of psychometric functions for simple gratings of various frequencies. In discussing some theoretical implications of our results, it will be convenient (although not necessary) to have an analytical expression for such psychometric functions. One particularly convenient expression can be visualized in terms of the models in Figs. 2 and 3. We assume that a simple grating is detected by only one channel (either model); that the noise is zero mean, unit-variance gaussian; and that the filter output is some function, $G(m)$, of the modulation of the simple grating. Then the theoretical detection probability, $P(Y|m)$, will have the form

$$P(Y|m)=1-\left[\frac{1}{(2\pi)^{\frac{1}{2}}}\int_{-\infty}^{K-G(m)}\exp\left(-\frac{x^2}{2}\right)dx\right](1-c), \quad (9)$$

where $K$ is the threshold level (observer's criterion). If $G(m)=am$, then

$$P(Y|m)=1-\left[\frac{1}{(2\pi)^{\frac{1}{2}}}\int_{-\infty}^{K-am}\exp\left(-\frac{x^2}{2}\right)dx\right](1-c). \quad (10)$$

The solid curves in Fig. 6 have the form of Eq. (10), where $K$, $a$, and $c$ are maximum-likelihood estimates of the results.[12] In 34 out of 41 cases, the results for simple gratings are adequately fitted (i.e., not rejected at the 0.05 level by the $\chi^2$ test for goodness of fit) by a function of the form of Eq. (10) with maximum-likelihood estimates for the parameters. Four of the remaining cases were unusual in that only on those days were the psychometric functions not monotonic functions of the contrast. In all of our figures, therefore, we shall fit the simple psychometric functions according to Eq. (10), using maximum-likelihood estimators of parameters.

In Eq. (10) the mean of the normal distribution is proportional to the modulation. Two other functional relationships were tried, with less satisfactory results. If the mean is made proportional to the square of the modulation, our results appear to deviate systematically from the predicted probabilities and the resulting fit is rejected at the 0.05 level of significance in 17 out of 41 cases. A logarithmic transformation of the form $G(m)=\log(b+m)$ can be made to fit the results in all cases where a linear fit is adequate. However, in almost all cases, the best fit is obtained with an arbitrarily large value of $b$, in which case the logarithmic transformation reduces to a linear one. Finally, if the guessing mechanism is abandoned, by arbitrarily setting $c=0$ in Eq. (10), the simple psychometric functions cannot be adequately fitted by the resulting equation. It is possible, of course, that with some other density function for the noise, the guessing mechanism would not be necessary.

On the assumption that $G(m)=am$, the estimated values of the guessing probability, $c$, are 0 in 17 out of 41 cases, and occasionally run as high as 0.09; they do not appear to vary systematically with the spatial frequency of the gratings. The criterion, $K$, also does not appear to vary systematically; its average value was approximately 5.5. As expected, the estimated value of $a$, the modulation-sensitivity parameter, does vary with frequency, as shown in Fig. 7. The points are based on results of our observer MS, whose

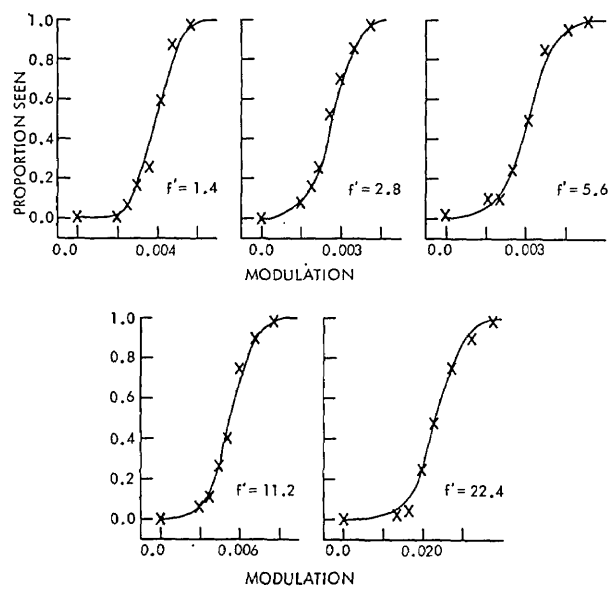


FIG. 6. Psychometric functions for simple gratings of various frequencies. Solid lines are fitted in accordance with Eq. (10). Frequencies are given in cycles/deg. Modulation scale is linear. Observer MS.

refractive errors were optically corrected; each point is the average of several estimates, obtained on different days. The curve is based on results reported by Campbell and Robson[5] in their Fig. 3. They measured modulation sensitivity by the method of adjustment, under stimulus conditions similar to our own. The curve has been displaced vertically to provide a good fit to the points.

### B. Detection of Complex Gratings

#### *1. Multiple-Channels Hypothesis*

In order to test the multiple-channel hypothesis, we performed an extensive series of experiments with $f=14$ cycles/deg and $f'$ taking on values in the range of 2.8 to 28 cycles/deg. Typical results for one observer are shown in Fig. 8; the results for the other observer are quite similar. In each frame we have plotted both the simple psychometric function for the frequency $f$ alone and the complex psychometric function. The simple psychometric functions have been fitted by Eq. (10) in accordance with the preceding section. The solid curves drawn through the complex psychometric functions are scaled versions of the simple psychometric functions, in accordance with the simplest separate-channels case of the multiple-channel hypothesis. In that case, we assumed that each channel detects only one of the components of the complex grating. Consequently, the probability of not detecting the complex grating is a constant fraction of the probability of not detecting the corresponding simple grating, as in Fig. 4(b). We have chosen the scaling factor that minimizes the value of $\chi^2$ in a test of independence to be discussed below. In Fig. 8, these scaled psychometric functions provide a good fit to the detection performance for complex gratings in all cases but two. The two cases

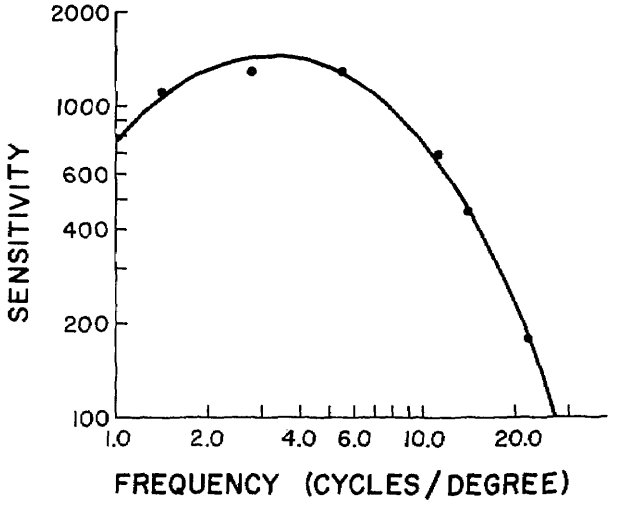


FIG. 7. Modulation sensitivity as a function of spatial frequency. The circles are average estimates of $a$ in Eq. (10) based on the results of observer MS. The solid curve is from Campbell and Robson,[16] Fig. 3, and has been displaced vertically to fit the circles.

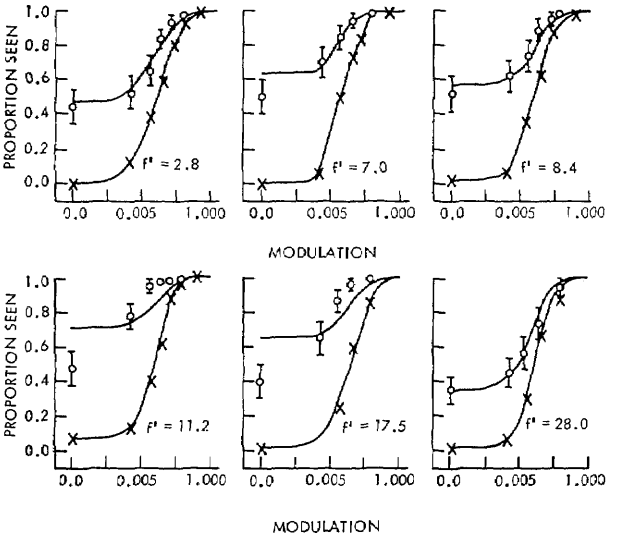


FIG. 8. Simple and complex psychometric functions for $f=14$ cycles/deg and various values of $f'$ (given in cycles/deg). The solid curves are fitted to the simple psychometric functions in accordance with Eq. (10). The solid curves fitted to the complex psychometric functions correspond to the multiple-channel model in the case where $f$ and $f'$ are detected by completely separate channels (see text). Vertical bars correspond to 95% confidence intervals. Observer MR.

in which the fit is clearly poor occurred where the components of the complex grating were closest in frequency ($f/f'=4/5$ or $5/4$).

In order to check on the tenability of the simplest form of the multiple-channel hypothesis without making any assumptions about the form of the simple psychometric functions, we applied a $\chi^2$ test of independence to our results.[13] Specifically, the trials on which the observer responded "no" in each experimental session were classified according to (a) the presence or absence of the stimulus component at frequency $f'$ and (b) the modulation of the component at frequency $f$. It can be shown that the assumption that $f$ and $f'$ are detected by completely separate and independent channels is equivalent to the hypothesis that these two ways of classifying "no" responses are independent. This hypothesis was subjected to a $\chi^2$ test of independence. For the results shown in Fig. 8, the independence hypothesis is rejected at the 0.05 level of significance only where $f/f'=4/5$ or $5/4$. In Table I, we have listed the probability of obtaining a $\chi^2$ value greater than that actually obtained in each of our experiments where $f=14$ cycles/deg, for both of our observers.

TABLE I. Probabilities from $\chi^2$ test of independence, for $f=14$ cycles/deg.

| | Frequency $f'$ (cycles/deg) | | | | | | | | | | |
|---|---|---|---|---|---|---|---|---|---|---|---|
| Observer | 2.8 | 7.0 | 7.0 | 7.0 | 8.4 | 8.4 | 8.4 | 11.2 | 11.2 | 17.5 | 28.0 |
| MS | 0.21 | 0.7 | 0.01 | 0.3 | 0.40 | 0.27 | 0.7 | 0.00 | 0.00 | 0.00 | 0.40 |
| MR | 0.73 | 0.08 | | | 0.28 | 0.01 | 0.45 | 0.00 | 0.00 | 0.00 | 0.64 |

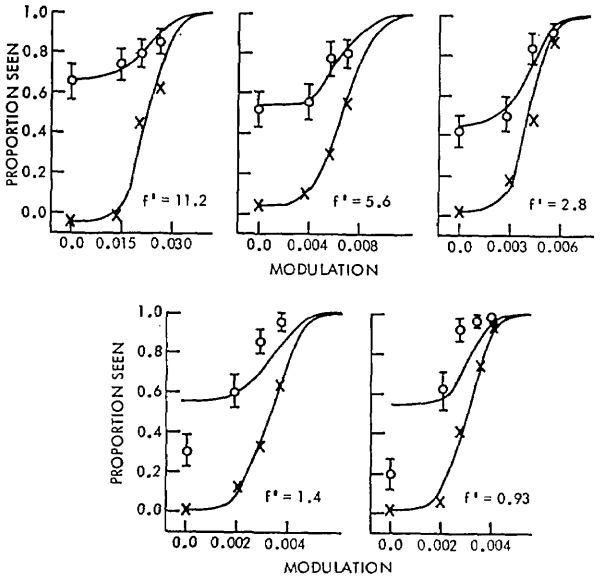


FIG. 9. Simple and complex psychometric functions for $f/f'=2$ and several values of $f'$ (in cycles/deg). Observer MS.

The independence hypothesis is consistently rejected at the 0.05 level of significance only where $f/f'=4/5$ or $5/4$. It is also rejected in one case where $f/f'=2$ and in one case where $f/f'=5/3$. These latter two cases were among those called unusual in the preceding section. On both days, either simple or complex psychometric functions or both were nonmonotonic functions of $m$. We considered this result to indicate erratic behavior.

Our results are thus generally consistent with the hypothesis that the two components of a complex grating, provided that their frequencies are sufficiently different, are detected by entirely separate and independent channels. The channel centered at 14 cycles/deg must be tuned narrowly enough so that it does not respond significantly to spatial frequencies differing by a factor of 2 or more. To investigate the generality of this result, we performed a series of similar experiments with different values for $f$ and with the ratio of $f$ to $f'$ kept equal to 2. The results from one subject are shown in Fig. 9. The results from the other subject are quite similar. Clearly, the independence hypothesis provides a good fit to the detection probabilities for the complex gratings, except at the two lowest values of $f$—2.8 and 1.86 cycles/deg. Table II shows that for both subjects the independence hypothesis can be rejected at the 0.05 level only for these two lowest frequencies.

TABLE II. Probabilities from $\chi^2$ test of independence, for $f=2f'$.

| | Frequency $f'$ (cycles/deg) | | | | | |
|---|---|---|---|---|---|---|
| Observer | 11.2 | 5.6 | 2.8 | 1.4 | 1.4 | 0.93 |
| MS | 0.54 | 0.22 | 0.66 | 0.00 | 0.00 | 0.00 |
| MR | 0.54 | 0.83 | 0.17 | 0.00 | 0.00 | |

However, even in the low-frequency range, the independence hypothesis cannot be rejected if $f$ and $f'$ are made sufficiently different, as can be seen from Fig. 10. Here we have plotted simple and complex psychometric functions for $f=2.8$ cycles/deg and $f$ to $f'$ ratios of 3 in one case and 2 in the other. It is clear from the figure (and substantiated by the $\chi^2$ test) that while the independence hypothesis provides a very poor fit in the 2 and 1 case, it provides a good fit in the 3 to 1 case.

### 2. *Single-Channel Hypothesis*

According to the two forms of the single-channel model set forth in the introduction, the complex psychometric function should be a leftward-shifted version of the simple psychometric function, when plotted against either $m^2$ or $m$. Figure 11 illustrates the failure of the predictions in a situation in which one of them should have held—two sinusoidal components with $f=14$ and $f'=2.8$ cycles/deg, superimposed in such a way that each peak and trough of the low-frequency component coincided with a peak and trough, respectively, of the high-frequency component. For this input, the response of a single linear spatial filter with symmetrical spread function should be proportional to exactly $am+a'm'$, where $a$ and $a'$ are constants that depend upon $f$ and $f'$. In the figure, the detection probabilities obtained from both observers are plotted on an abscissa linear in $m$ as well as on one linear in $m^2$. The dotted curves are the simple psychometric functions shifted laterally in accord with a minimum $\chi^2$ criterion. In every case, they provide a very poor fit indeed to the detection probability obtained for the complex grating $[P(\chi^2)\ll 0.001]$.

It will be recalled that, for this situation, we could not reject the independence hypothesis based on the simplest form of the multiple-channel model. In general, whenever a pair of related simple and complex psychometric functions could be fitted by the independence

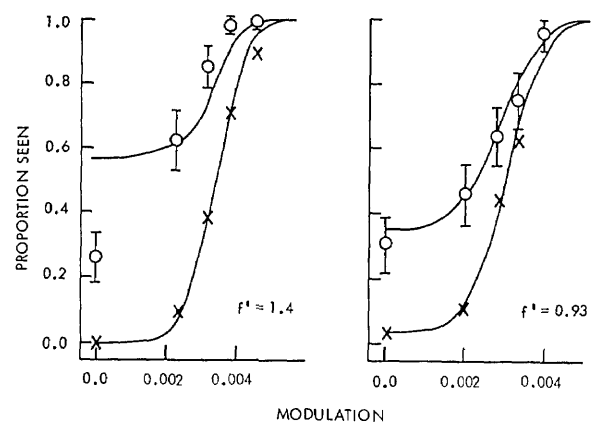


FIG. 10. Simple and complex psychometric functions for $f=2.8$ and $f'=1.4$ and 0.93 cycles/deg. Observer MS.

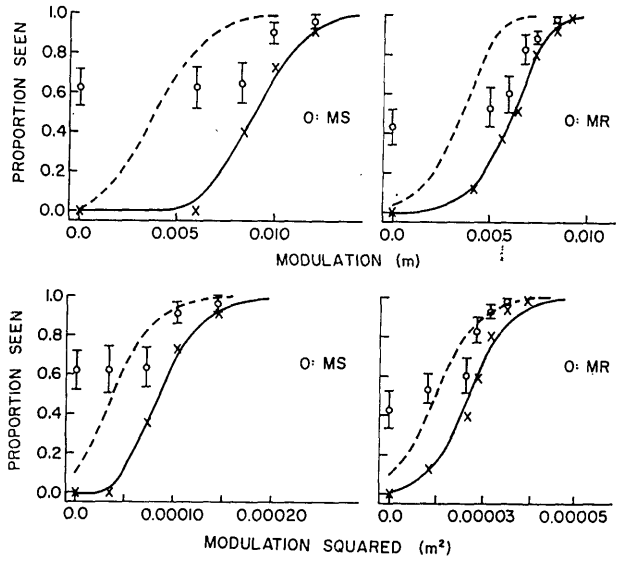


FIG. 11. Simple (×) and complex (○) psychometric functions for $f=14$ cycles/deg and $f'=2.8$ cycles/deg, plotted on abscissa linear in $m$ (upper panels) and linear in $m^2$ (lower panels). As before, Eq. (10) has been fitted to the simple psychometric function. The curves were then displaced leftward to provide the best fit possible to the complex psychometric functions, in accordance with two versions of a single-channel model.

hypothesis, they could not be fitted by the peak-to-trough or average-power versions of the single-channel model. The converse was also generally true. But, whereas we would expect the independence hypothesis to fail when $f'$ is close to $f$, even if the multiple-channels model were correct, there is no reason why the single-channel model, if true, should fail to hold when $f'$ is not close to $f$.

We must therefore reject at least those versions of a single-channel model that we have considered. Conceivably, there may exist other versions of a single-channel model that can account for our results. We have been unable to discover them.

## DISCUSSION

All of our results are clearly consistent with the model of the visual system presented in Fig. 3. This model was based on the assumptions that

(1) the human visual system contains several sensory channels, each selectively sensitive to a different, moderately narrow range of spatial frequencies;

(2) the outputs of the various channels are stochastically independent;

(3) the output of each channel is passed through a separate threshold device;

(4) a grating is detected when the critical level of at least one of the threshold devices is exceeded, or when a "yes" is generated by an independent guessing mechanism.

Our test of the simplest case of the multiple-channel hypothesis did not depend on any other assumptions about the channels. In order to gain some appreciation of more specific characteristics of these channels, such as the shape of their frequency-response curves, and to compare our results with existing physiological and psychophysical data, it is necessary to deal with the more general case wherein the separation between $f$ and $f'$ may or may not be large with respect to the bandwidths of the visual channels. Unfortunately, to do so requires additional assumptions—assumptions not rigidly constrained by existing data. On the basis of a particular set of such assumptions, we have estimated for the channel most sensitive to 14 cycles/deg its relative sensitivity to other frequencies. The assumptions and estimation procedures are described in the Appendix. The resulting relative-sensitivity coefficients are plotted in Fig. 12, and represent our tentative conclusion about the shape of the frequency-response curve of one of the channels. Note its narrowness; sensitivity is down by about $\frac{1}{3}$ only 20% away from the peak frequency.

### A. Relevant Electrophysiological Evidence

We now turn briefly to a consideration of the possible neural substrate of the spatial-frequency filters that we have inferred from our psychophysical results. It is tempting to suppose that retinal ganglion cells could be that substrate. An ordered array of such ganglion cells, with widely overlapping receptive fields of the antagonistic center-surround variety, can act as a spatial-frequency filter. The location and bandpass region of such a filter would be a function of the

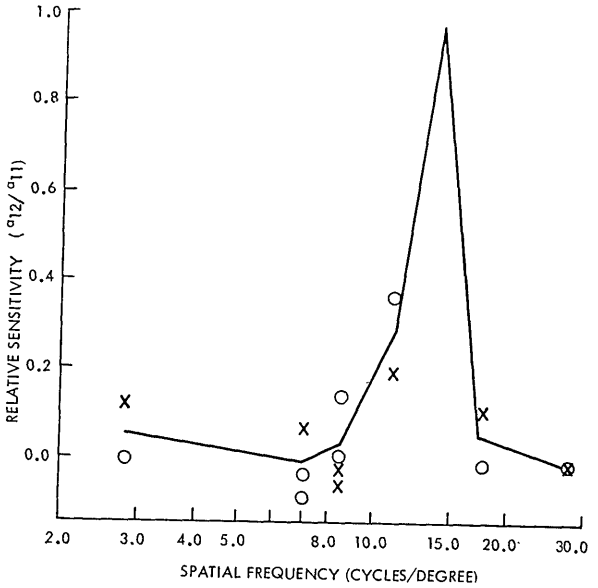


FIG. 12. Relative sensitivity as a function of frequency for the channel most sensitive to $f=14$ cycles/deg. ×'s are based on data from observer MR, ○'s from observer MS. Solid lines join mean values at each frequency tested. (See Appendix.)

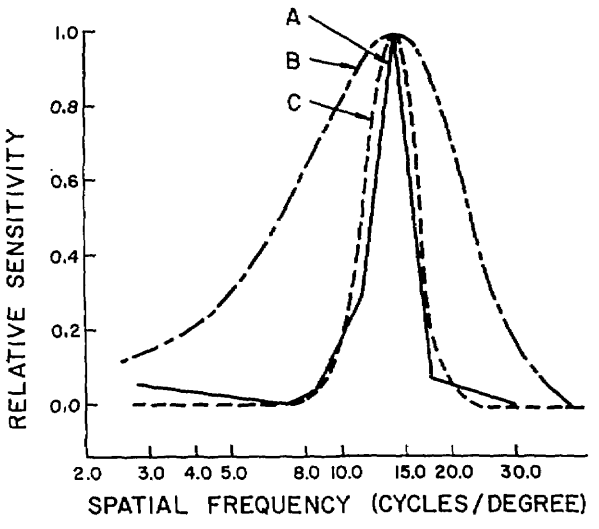


FIG. 13. A. Mean values of relative sensitivity from Fig. 12. B. Narrowest frequency-response function described by Eq. (11). C. Tenfold cascade of the system described by B.

dimensions of the receptive fields. From the work of Enroth-Cugell and Robson,[6] among others, we know that receptive fields of different dimensions coexist within the same region of the cat and monkey retina. The responses of each set of cells with like-sized receptive fields might then be the neural substrate for the output of each of the spatial-frequency filters required by the multiple-channels model.

However, quantitative considerations lead us to reject this simple possibility. The responses of single optic nerve fibers in the cat[6,14] and monkey[7] can be adequately fitted by assuming concentric center and surround summating regions, each with a gaussian point-spread function, whose outputs subtract arithmetically. These assumptions lead to a frequency-response function of the form

$$S(\nu)=k\pi\{k_c r_c^2 \exp[-(\pi r_c \nu)^2] - k_s r_s^2 \exp[-(\pi r_s \nu)^2]\}. \quad (11)$$

The equation actually describes a family of curves whose position and form depend on the values of the parameters $r_s$, $k_s$, $r_c$, and $k_c$. The narrowest member of this family, centered on 14 cycles/deg, is plotted (curve B) in Fig. 13, together with the solid curve (labeled A) redrawn from Fig. 12. Quite clearly, the tuning curve that we derived from our results by applying the two-channel model cannot be accounted for by the known quantitative properties of retinal ganglion cells in cat and monkey.

In principle, there are several ways in which narrowly tuned filters could be generated from broader ones. One way is by cascading. The frequency-response function of a cascade of $n$ identical linear filters is the frequency-response function of one of them raised to the $n$th power. If the retinal interactions described by curve B in Fig. 13 recur at 10 successive stages in the visual system, the resulting function will have the form of the dashed curve (labeled C) in Fig. 13. This curve fits quite well the relative sensitivities estimated from our results, represented by curve A. To date, electrophysiological investigation of the geniculate and visual cortex of cat and monkey[7,15] have failed to reveal any such high order of cascading, or such narrowly tuned frequency-response curves.

### B. Relation to Other Psychophysical Evidence

Several recent psychophysical studies have considered the spatial-frequency selectivity of the visual system. Blakemore and Campbell[9] have shown that adaptation to a grating of one spatial frequency causes threshold elevation for test gratings of frequencies close to the adapting frequency. They found that plots of percent threshold elevation vs frequency of test grating could be fitted by the square of a function of the form of Eq. (11). As indicated in Fig. 13, the frequency-response function that we have estimated from our results is much narrower than the function in Eq. (11). However, Blakemore and Campbell's curves cannot be related quantitatively to underlying frequency-response curves without making additional assumptions, which can be readily tested by further experiments.

Campbell, Nachmias, and Jukes[16] have measured discrimination limits for spatial frequency and have found that over a wide frequency range, $\Delta f/f$ is approximately 4%. Of course, this does not imply that the relative bandwidth of the channels is of the same order. In a perfectly noise-free situation, for instance, as long as there are different channels tuned to frequencies 4% apart, then these two frequencies can be discriminated, regardless of the channel bandwidth.

Graham and Nachmias[17] determined threshold contrast for related simple and complex gratings with $f/f'=3$. The relative phase between the two sinusoidal components, $\phi-\phi'$, was set to either 0 or $\pi/2$. They showed that their results contradict the single-channel model (peak-to-trough detector) although they are compatible with the multiple-channel model (separate-channels case).

### C. Field-Size Limitations

In discussing the form of these spatial-frequency filters, we must consider the effects of limited field size on our measurements. In order to get an accurate measurement of the frequency-response function for a filter whose nominal bandwidth is $W$, input signals must be used whose extent is large[18] compared with $2/W$. Consider the filter that is a 10-fold cascade of the one whose frequency response is given by Eq. (11). This filter has a bandwidth comparable to that of our estimated frequency-response curve, as is shown in Fig. 13. The half-power bandwidth of this filter is approximately 3.5 cycles/deg. Thus, for accurate

measurements of such a filter, we must use stimuli whose spatial extent is large compared with $2/3.5=0.6$ deg. The horizontal dimension of our field was about four times this value, so that the error imposed by field-size limitation should be small, for this 14-cycles/deg channel. Furthermore, any error imposed by field limitation will be in the direction of broadening the apparent frequency-response curve of the channel, so that we can again say that the 14-cycles/deg channel is no wider than the one we have shown in Figs. 12 and 13.

We have accumulated enough data to estimate more than two points of the frequency-response function only for the channel centered at 14 cycles/deg. However, in the experiments in which $f/f'$ was held equal to two, we found that the two components of a complex grating can be assumed to be detected by separate and independent channels for $f$ between 5.6 and 28 cycles/deg. In the 14-cycles/deg case we found that the independence hypothesis was rejected for $f/f'=4/5$ or $5/4$. Figure 13 shows that the (average) relative sensitivity of the 14-cycles/deg channel at $f'=4/5f$ is approximately 0.3. On the basis of these calculations, then we can argue that the relative sensitivity of channels centered in the range 5.6–28 cycles/deg must be less than about 0.3 at frequencies that differ by a factor of 2 from the center frequency of the channel.

In the cases $f/f'=2$ with $f=2.8$ (or 1.86) cycles/deg we found that the independence hypothesis was rejected, whereas for $f=2.8$ and $f'=0.93$ cycles/deg, it was not rejected. In considering these results, we must certainly take into account the effects of field-size limitation. Because this limitation can only broaden the apparent frequency-response function of a given channel, it does not invalidate any finding of independent detection for a pair of frequencies. Thus, our evidence for the existence of separate channels below 2.8 cycles/deg is not affected by any field-size limitation. Our results would seem to indicate, however, that the channels centered at 2.8 cycles/deg and below are more broadly tuned than are the higher-frequency channels. The relative bandwidth of the 14-cycles/deg channel is about $3.5/14=0.25$. If this relative bandwidth at 2.8 cycles/deg would be $0.25\times2.8=0.7$ cycles/deg, we would therefore need a field large compared with $2/0.7=2.86°$. Our field is thus too small to estimate the frequency response of the 2.8-cycles/deg channel, and the apparent broadening of the tuning could be a field-size effect.

In order to test this notion, we performed an additional experiment in which $f=11.2$ and $f'=5.6$ cycles/deg, and the gratings were reduced to 0.54° on a side. (Because $0.54°=2.2°\times1.4/5.6$, the relative bandwidth of these stimuli are the same as those in the 1.4-cycles/deg, 2.2°-field case.) The independence hypothesis could not be rejected in this experiment. We have thus demonstrated that the apparent broadening of the low-frequency channels cannot be solely a field-size effect.

## CONCLUSION

Our results provide strong evidence for the existence of channels in the human visual system that are selectively sensitive to different ranges of spatial frequencies and whose outputs are detected independently. Therefore, in a detection situation, the visual system cannot be considered to be a single spatial filter.

## ACKNOWLEDGMENTS

This paper is based on experimental work performed at The Physiological Laboratory, Cambridge, England. MBS was a National Science Foundation Postdoctoral Fellow on assignment from the Navy Underwater Sound Laboratory. JN was on leave of absence from the University of Pennsylvania and was partially supported by research grant No. NB06050 from the U. S. Public Health Service. JGR was in receipt of a Medical Research Council grant.

We gratefully acknowledge the technical and psychophysical assistance of M. Rodel during the experimental phase of this research. We are also indebted to Dr. G. Sperling, Dr. J. Krauskopf, and D. Aldrich for useful comments on an earlier draft of this paper.

## APPENDIX: ESTIMATING THE FREQUENCY-RESPONSE CURVE OF ONE CHANNEL

### Assumptions

(1) In the model illustrated in Fig. 3, we can neglect the contribution of all channels but two to the detection of our complex gratings—the channel most sensitive to frequency $f$ and the one most sensitive to $f'$. For subsequent notational convenience, we will rename $f$ as $\nu_1$, and $f'$ as $\nu_2$. (2) The noise added to the output of each filter is zero-mean, unit-variance gaussian. (3) The criterion levels of the two threshold devices are the same ($K_1=K_2=K$). (4) The output of each filter is a linear combination of the modulations of the stimulus gratings. This assumption will be discussed further in a later section of this Appendix.

### Estimation Procedure

On the above assumptions, the probability of not detecting a complex grating is

$$P(N\,|\,m,m')=\left[\frac{1}{(2\pi)^{\frac{1}{2}}}\int_{-\infty}^{K-a_{11}m_1-a_{12}m_2}\exp(-x^2/2)dx\right]\times\left[\frac{1}{(2\pi)^{\frac{1}{2}}}\int_{-\infty}^{K-a_{21}m_1-a_{22}m_2}\exp(-x^2/2)dx\right](1-c), \quad \text{(A1)}$$

where $a_{ij}$ is the sensitivity of channel $i$ to frequency $\nu_j$,

and $m_j$ is the modulation of the sinusoid at frequency $\nu_j$. It is easy to derive the relationships between maximum-likelihood estimators for all the parameters of Eq. (12) and our results for simple and complex gratings. Further, it can be shown that when $a_{21}/a_{11}<\frac{1}{2}$, the contribution of channel 2 to the detection of a simple grating at frequency $\nu_1$ is negligible. This result is due to the rapid rise of the simple psychometric functions. (The proportion of simple gratings seen increases from 5% to 95% for less than a twofold increase of $m_1$.) In order to simplify the computations, we have therefore assumed that a simple grating at frequency $\nu_1$ is detected by channel 1 only. For a simple grating at frequency $\nu_1$, Eq. (A1) then reduces to Eq. (10) with $a=a_{11}$. We have used our simple-grating results to estimate $K$, $a_{11}$, and $c$ by the probit-analysis techniques described by Finney.[12] With these estimates of $K$, $a_{11}$, and $c$ for each experimental session, we then found maximum-likelihood estimates of $a_{12}$, $a_{21}$, and $a_{22}$. The Newton–Raphson method was used to find the roots of the three equations defining these estimates.[19]

In Fig. 12 relative sensitivity ($a_{12}/a_{11}$) is plotted as a function of $\nu_2$ for the channel tuned to $\nu_1=14$ cycles/deg. Relative sensitivity was calculated from our results by the method outlined above. The plotted points are based on data from both observers. Solid lines connect the average values of relative sensitivity at each frequency used. No points are included for which the fit of Eq. (10) to the simple psychometric function is rejected by a $\chi^2$ test at or beyond the 0.02 level.

### Relation to Peak-to-Trough Detector

In calculating the frequency-response function from our data, we assumed that the output of filter $j$ is a linear combination of the modulations, namely, $a_{j1}m_1+a_{j2}m_2$, for all values of $\nu_1$ and $\nu_2$. No restriction was placed on the sign of the sensitivity coefficients and, in fact, the maximum-likelihood estimates of the sensitivity coefficients $a_{j1}$ and $a_{j2}$ were sometimes of opposite sign.

This assumption is similar to another, which though perhaps more plausible, is considerably less tractable mathematically—namely, that each channel is a peak-to-trough detector. For the relative phases between sinusoidal components which we used in our complex gratings, the peak-to-trough assumption would lead to identical estimates in certain cases—when $\nu_2=(1/5)\nu_1$ or $(3/5)\nu_1$, and when all $a_{ij}$, as estimated by our assumption, are of the same sign. In all other cases, the peak-to-trough assumption would lead to higher estimates of relative sensitivity ($a_{12}/a_{11}$). The magnitude of the discrepancy is least for $\nu_2=(5/4)\nu_1$ or $(4/5)\nu_1$, and greatest for $\nu_2=(1/2)\nu_1$ or $2\nu_1$. However, even in the last case, sample calculations show that relative sensitivity is unlikely to be greater than 0.15.

### REFERENCES


* Some of this work was presented at the October 1969 meeting of the Optical Society of America [J. Opt. Soc. Am. **59**, 1538A (1969)].

† Present address: Department of Biomedical Engineering, Johns Hopkins University School of Medicine, Baltimore, Md. 21205.

[1] O. H. Schade, J. Opt. Soc. Am. **46**, 721 (1956).

[2] H. deLange, J. Opt. Soc. Am. **48**, 777 (1958).

[3] J. G. Robson, J. Opt. Soc. Am. **56**, 1141 (1966).

[4] F. Ratliff, *Mach Bands: Quantitative Studies on Neural Networks in the Retina* (Holden-Day, San Francisco, 1965).

[5] F. W. Campbell and J. G. Robson, J. Physiol. (London) **197**, 551 (1968).

[6] C. Enroth-Cugell and J. G. Robson, J. Physiol (London) **187**, 517 (1966).

[7] F. W. Campbell, G. F. Cooper, J. G. Robson, and M. B. Sachs, J. Physiol. (London) **204**, 120 (1969).

[8] A. Pantle and R. Sekuler, Science **162**, 1146 (1968).

[9] C. Blakemore and F. W. Campbell, J. Physiol (London) **203**, 237 (1969).

[10] C. Blakemore and P. Sutton, Science **166**, 245 (1969).

[11] Whenever $f/f'$ can be expressed as a ratio of odd integers, then there is some value of $(\phi-\phi')$ for which the largest peak-to-trough difference in the input complex waveform will be equal to exactly $2L_0(m+m')$. The corresponding peak-to-trough value for the output of the single channel (assuming a symmetrical spread function) will be proportional to $(am+a'm')$. Hence, for a peak-to-trough detector, the functions $G$ and $G'$ in Eq. (3) are linear in $m$ and $m'$, respectively. For other values of $f/f'$, the largest peak-to-trough difference in the luminance waveform will be less than $2L_0(m+m')$ no matter what the phase of the component sinusoids.

[12] D. J. Finney, *Probit Analysis* (Cambridge U. P., England, 1964), Appendix II.

[13] A. M. Mood and F. A. Graybill, *Introduction to the Theory of Statistics. 2nd ed.* (McGraw-Hill, New York, 1963), Ch. 12.

[14] R. W. Rodieck and J. Stone, J. Neurophysiol. **28**, 833 (1965).

[15] F. W. Campbell, G. F. Cooper, and C. Enroth-Cugell, J. Physiol (London) **203**, 223 (1969).

[16] F. W. Campbell, J. Nachmias, and J. Jukes, J. Opt. Soc. Am. **60**, 555 (1970).

[17] N. Graham and J. Nachmias, Vision Res. **11**, 251 (1971).

[18] R. B. Blackman and J. W. Tukey, *The Measurement of Power Spectra* (Dover, New York, 1958).

[19] D. D. McCracken and W. S. Dorn, *Numerical Methods and Fortran Programming* (Wiley, New York, 1964), Ch. 5.